Impact of the Two-Slope Path Loss Model in the Service Quality of 4G and 5G Small Cells

Rui R. Paulo and Fernando J. Velez
Instituto de Telecomunicações and Universidade da Beira Interior
DEM – Faculdade de Engenharia
Covilhã, Portugal
ORCID: 0000-0002-8541-6675, 0000-0001-9680-123X

***Abstract*—Together with cell-free networks, small cells enable ultra-dense networks in 5G. Although small cell networks will be part of heterogeneous networks, the comparison of service quality of urban micro (UMi) small cells between 4G and 5G second phase scenarios is still of great relevance. Usage of video (VID), is considered. Quality of service (QoS) is determined by considering a packet loss ratio (PLR) lower than 2%, for different sub-6 GHz frequency bands. The aim is to compare the system capacity between 4G and 5G enhanced mobile broadband in different bands. ITU defined two UMi cell scenarios for urban micro cells that consider two-slope (TS) path loss models (PLMs). In this work, we have included TS-PLMs into the LTE-Sim (4G) and 5G-air-simulator. The service quality and system performance bands have then been evaluated. Results shows that it is possible to support more user terminals (UTs) with 5G (up to 26 UTs) than with 4G (10 UTs only). When PLR<2%, the average delay decreases and the average goodput increases when 5G is considered. The maximum average goodput also increases with 5G.**

***Index Terms*—5G, 4G, UMi_A, UMi, dual-slope, performance evaluation, small-cell networks, line of sight, saturation level.**

I. Introduction

The incessant evolution of the mobile system has always brought new challenges to the research community, standard development organizations, regulators and other market players [1], [2]. One of the many challenges is how to deal with the exponential increase in the demand of data traffic and the increase in the number of users as well by the springing up of new broadband applications and services [3], [4]. In 5G, there is a need to support different kinds of user terminals (UTs), technologies and services. This is driving to a revolution on technology to achieve highly efficient 3GPP systems of high-performance [5], [6]. To deal with this demand, not only in terms of total traffic but also per deployment area, small cells are being added to the existing networks [7].

3GPP defines nine scenarios that have performance requirements that aim to support high data rates and traffic densities [5], [6]. In these scenarios, the UT speed varies from stationary to UTs that are in airplanes, with velocities up to 1 000 km/h. The coverage in theses scenarios are, in some cases, provided by small cells, e.g., the dense urban, indoor hotspot and UTs that are traveling inside high speed vehicles. UTs can consume multimedia services and applications with advanced quality of experience (QoE). Quality of service (QoS) expresses the network behavior by metrics as the packets loss, delay between the source and destination nodes, which includes effects of propagation and jitter. The calculation of the QoE could be determined by measuring the user experience or by determining the QoS that can be applied by using conceptual functions to predict the QoE [8].

Another characteristic of 5G is to support multiple access technologies. This means that it has to be capable to support 4G and other previous technologies. This legacy is shared by the 3GPP Release 17 and Release 18 [9], [10].

The ITU-R published two reports that provide the guidelines to evaluate radio interfaces [11], [12]. As it was published first, report [11] has often been applied to studies in 4G radio interfaces. On the other hand, Report [12] is becoming to be considered for 5G radio interfaces. These evaluations of the radio interfaces has to deal with the fact that the power of wireless signal transmissions gradually degrades over distance [13]. In [11], [12] these losses are expressed by dual-slope path loss models (DS-PLMs) in urban micro cell scenarios.

Although the impact of DS-PLMs has been studied, like in [13]–[15], these works did not provide QoS results derived from numerical simulations.

The main contributions of the paper can be summarized as follows:

- As non-standalone 5G New Radio coexists with 4G, a comparison of the behavior of both technologies is in order while considering the ITU-R reports mentioned above and taking into account the end-user performance expectations, as defined in [16];
- As the system capacity depends on the target values for the Packet loss Ratio (PLR) and average delay, numerical simulations will consider the system saturation;
- Performance evaluation beyond the system saturation turning point will enable to determine if the defined QoS requirements, established in [16], do not cause wasting of system resources.

The rest of the paper is organized as follows. In Sec. II the physical and radio parameters are presented, the path

This work was supported by FCT/MCTES through national funds and when applicable co-funded EU funds under the project UIDB/50008/2020, COST CA20120 INTERACT and SNF Scientific Exchange - AISpectrum (project 205842), ORCIP (22141-01/SAICT/2016) and TeamUp5G. TeamUp5G project has received funding from the European Union's Horizon 2020 research and innovation programme under the Marie Skłodowska-Curie project number 813391.

loss models considered by ITU are also discusses. Simulation parameters are also introduced. Sec. III presents the results for the average packet loss ratio, average delay and number of supported UTs for PLR<2%. Sec. IV presents results for the average goodput and average delay beyond PLR<2%. Finally, conclusions are drawn in Sec. V.

II. UMi Path Loss Model and Simulation Parameters

The path loss modeling in this work is two-fold. For 4G, we consider the urban micro (UMi) cell scenario, as defined in [11]. For 5G, we also consider an urban micro cell scenario, as defined in [12] Yet, here the urban micro cell scenario has two variants, referred as "model A" (UMi_A) or "model B" (UMi_B). UMi_A is applied for frequency bands ranging from 0.5 GHz to 6 GHz, while in UMi_B frequencies range from 0.5 GHz to 100 GHz. We have compared three central frequency bands: the 2.6 GHz, 3.5 GHz and 5.62 GHz. In 5G these bands correspond, to the n7, n78, and n46 operating bands, respectively, as defined in [17]. Hence, the UMi_A cell scenarios as assumed.

A. Physical and Radio Parameters

From the test environments in [11], [12] we have considered a scenario with one layer of 19 hexagonal small cells with reuse pattern three, as shown in Fig. 1. Each color represents

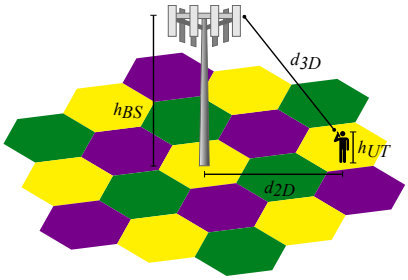

Fig. 1. UMi_A LoS microcells simulation scenario with reuse pattern three. Definition of gNB and user's heights and distances for outdoor users. Partially adapted from [12].

a single tier, and for each tier is considered 20 MHz of bandwidth. Users are in line-of-sight (LoS) to the base station (BS) antenna. The packet scheduling occurs at the BS. In this work we have considered the M-LWDF scheduler that is a QoS-aware scheduler [18]. The BS and UT antennas are assumed to be outdoors, and well below the top of the surrounding buildings. We have considered the BS antenna effective height is 10 m and for the UT an effective height antenna of 1.5 m. The transmitter power for UTs is 23 dBm. According to the considered frequency band, the transmitter power at the small cell varies. For 2.6 GHz it is 40 dBm, while for the 3.5 GHz and 5.62 GHz, it is 42.25 dBm and 46.70 dBm, respectively. The distance between the BS and the UT at the horizontal plane, as shown in Fig. 1 is defined as d_{2D}. d_{3D} is the distance between the BS and the UT antennas. The h_{BS} and h_{UT} are the antenna heights at BS and UT, respectively.

B. UMi and UMi_A Path Loss Models

One-slope (OS) path loss models (PLMs) are simple models that tend to fail into capturing short-distance path loss behavior [19]. In urban environments like the UMi and UMi_A we can observe an profusion of different types of obstacles. Consequently, when the distance between the transmitter and the receiver nodes increases the attenuation also increases. In these environments, the OS-PLMs tends to be limited to capture these effects. In order to increase the accuracy of the PLMs and also to better capture the link variations along the distance the two-slope (TS) PLMs have been adopted by the research community [20]. When TS-PLMs are compared to the OS-PLMs, it is observed that TS-PLMs present advantages to more closely matches empirical data [21].

ITU for UMi and UMi_A considers the following TS-PLMs. Eq. 1 presents the path loss, PL, between the 10 m cell radius, R, and UTs located up to the breakpoint distance, $d^{'}_{BP}$, as follows:

$$\begin{aligned} PL_a^{\text{UMi/UMi\_A}}(d) =& 22.0\log_{10}(d) + 28.0 + 20\log_{10}(f_c), \\ & 10\,\text{m} < d_{2D} < d^{'}_{BP}, \end{aligned} \tag{1}$$

f_c is the frequency given in GHz. In both ITU reports [11], [12] this Eq. is identical, the only difference is in the distance between the UTs and the BSs, for the UMi $d = d_{2D}$ and for UMi_A $d = d_{3D}$, in meters. With the introduction of the 3D modeling is possible to exploit elevation dimensions and becomes possible to make a combination of geographic environment and usage scenario that reflects the test environment.

For distances longer than the $d^{'}_{BP}$, the PL for the UMi scenario, and according to [11], is calculated by considering Eq. 2, as follows:

$$\begin{aligned} PL_b^{\text{UMi}}(d_{2D}) =& 40.0\log_{10}(d_{2D}) + 7.8 \\ & - 18\log_{10}(h_{BS} - 1.0) \\ & - 18\log_{10}(h_{UT} - 1.0) + 2\log_{10}(f_c), \\ & d^{'}_{BP} < d_{2D} < 5000\,\text{m}. \end{aligned} \tag{2}$$

For UMi_A, according to [12], the PL is defined as follows:

$$\begin{aligned} PL_b^{\text{UMi\_A}}(d_{3D}) =& 40.0\log_{10}(d_{3D}) + 28 + 20\log_{10}(f_c) \\ & - 9\log_{10}\left(\left(d^{'}_{BP}\right)^2 + (h_{BS} - h_{UT})^2\right), \\ & d^{'}_{BP} < d_{2D} < 5000\,\text{m}. \end{aligned} \tag{3}$$

Apart from the clear differences between Eq. 2 and Eq. 3, it is important to highlight the following: Eq. 2 accounts the antennas effective heights at the BS and the UT, and considers the d_{2D} distance; Eq. 3 accounts the antenna heights and considers the d_{3D} distance. The effective antenna heights is defined for the UMi and UMi_A, as the antenna heights minus 1 meter.

As a consequence, the $d^{'}_{BP}$, is computed as follows

$$d^{'}_{BP} = \frac{4(h_{BS} - 1.0)(h_{UT} - 1.0)f_c}{c}, \tag{4}$$

where c is the propagation velocity in free space (and is equal to the speed of light, i.e., $\approx 3 \times 10^8$ m/s). The d'_{BP} is 156 m, 210 m and 337.2 m for 2.6, 3.5 and 5.62 GHz respectively (h_{BS} = 10 m and h_{UT} = 1.5 m).

C. Simulation Parameters and Simulators

To study the UMi small cell scenario we have upgraded LTE-Sim [22]. LTE-Sim is an open-source framework that simulates LTE-Advanced networks. Since developers of the simulator did not consider any DS-PLM, we made an upgrade to the simulator to consider the UMi scenario and PLM of [11].

To study the UMi_A cell scenario, we have upgraded the 5G-air-simulator [23]. According to its authors, 5G-air-simulator is an open-source and event-driven tool modeling the key elements of the 5G air interface, from a system-level perspective. This simulator considers a numerology 0, corresponding to a subcarrier spacing of 15 kHz, a number of subframes per radio frame of 10 and a frame duration of 10 ms. The simulator, as it is available by its authors, did not include the UMi_A cell scenario. Our contribution to the simulator has been to implement the UMi_A in LoS scenario. By extracting values from [12] for this implementation, we have considered the mean penetration loss equal to 9 dB, with a standard deviation equal to 5 dB. For a LoS probability equal to one, the shadow fading is equal to 3 dB, and the shadowing correlation distance is considered 10 m. We freely make available the upgrade version of the LTE-Sim and 5G-air-simulator under the GPLv3 license in [24], [25].

The same multimedia application was considered in both scheduler. The application is a video (VID) flow with a bit rate of 3.1 Mb/s, and the flow duration is 40 s.

III. Results at the Saturation Level

We have considered the 3GPP TS 22.105 [16] to determine the system saturation for VID flows. System saturation could be determined by regarding a PLR<2% or by a maximum delay of 150 ms. The simulation duration for 4G and 5G is 46 s. The values of cell radii, Rs, vary from 0.02 km up to 1 km. The number of R simulated is higher in 5G. The first simulations for each value of R started with one user. In order to get statistical significance, 50 simulations have been run, then the average PLR has been determined. If the average PLR is not higher than 2%, one more user is added and 50 new simulation are run. It is a worth noting that, the xx axis present different dimensions, between 4G and 5G, in different view charts. Results are presented in average terms, with a 95% confidence interval.

A. Average Packet Loss Ratio

As the erroneous packets are discarded, the packet loss ratio (PLR) is the percentage of packets that did not reach their destination from the total transmitted packets. Results for the PLR in 4G and 5G are presented in Fig. 2. The red line indicates the PLR = 2%. For both technologies the behavior is the same. However, the average PLR increases faster for the 4G technology, as shown in Figs. 2a, 2c and 2e, compared to 5G, as shown in Figs. 2b, 2d and 2f.

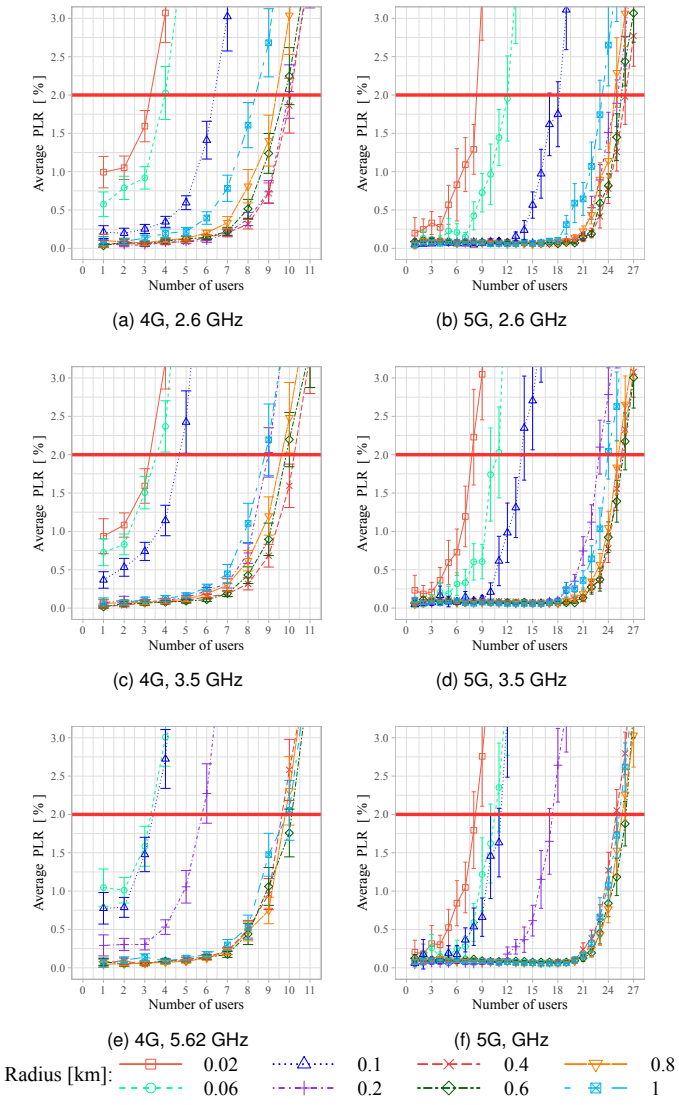

Fig. 2. Results for the average PLR as a function of the number of users with R as a parameter for different frequency bands.

For most of the values of R, initially, when the number of UTs increases the PLR increases almost linearly. Then it starts to increase exponentially. It is also visible, for shorter Rs and the same number of UTs, the average PLR start to increase faster than for longer Rs. For the longer Rs, the average PLR starts to increase slower. For 4G, and values of R around 700 m (depending of the frequency band) and the same number of UTs, the average PLR starts to increase faster. For 5G, in the 2.6 GHz frequency band, the average PLR starts to increase faster for Rs higher than 400 m. When the frequency band is 3.5 GHz, the same effect is observed for Rs longer than 700 m, while for the 5.62 GHz frequency band the same behavior occurs for Rs longer than 800 m.

B. Average Delay

After the average PLR is determined, by discarding values for the number of UTs corresponding to PLRs that are equal or higher than 2%, the average delay is determined. Results are presented in Fig. 3. These values of average delay are the

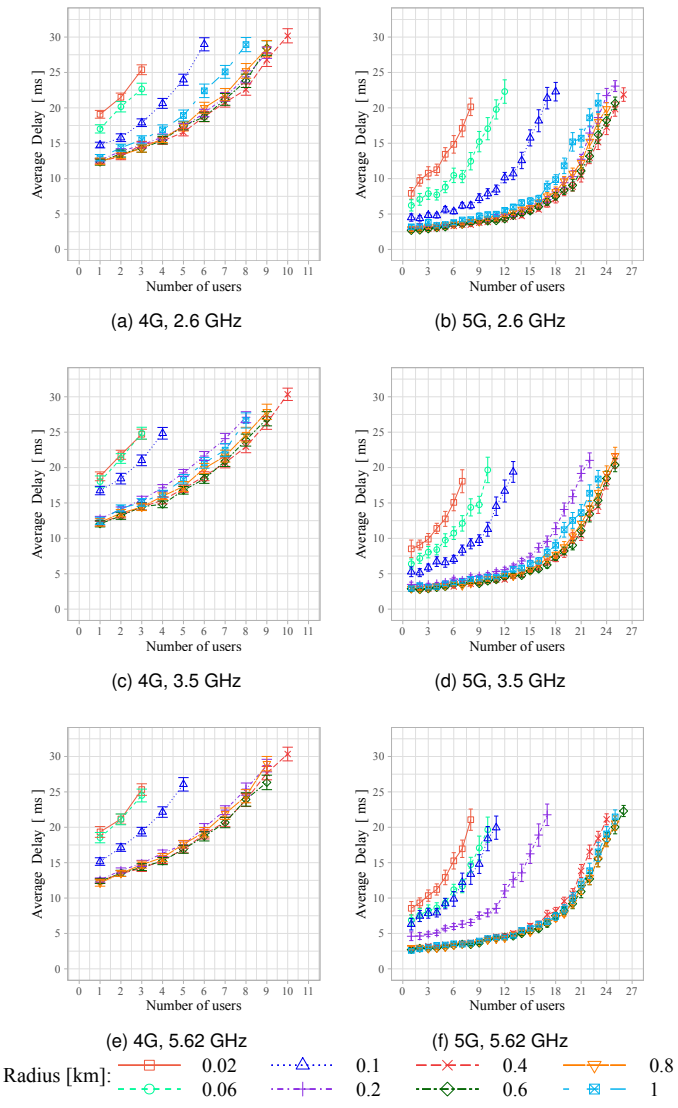

Fig. 3. Results for the average delay, as a function of the number of users, with R as a parameter, for different frequency bands, for PLR<2%.

values corresponding up to the system saturation. None of the obtained average delays is longer than the 150 ms (appointed by 3GPP).

In general, for all values or R and supported users, the average delay is shorter with 5G. For 4G the maximum average delay is between 30 ms and 32.5 ms, while for 5G that is between 22.5 ms and 25 ms, a decrease of around 7.5 ms.

It is also worthwhile to observe that, for the lowest number of supported users, the average delay in 4G is also longer than with 5G. While for 4G the minimum average delay is around 12.5 ms, in 5G, it is around 2.5 ms, a decrease of around 10 ms.

C. Supported Users

After determining the average PLR and average delay, it is possible to determine the number of supported users (UTs). The number of supported UTs are presented in Tab. I for each frequency band in 4G and 5G. Is important to emphasize that:

TABLE I
NUMBER OF SUPPORTED USERS FOR 4G AND 5G.

	4G			5G		
	Frequency Bands [GHz]					
Radius [km]	2.6	3.5	5.62	2.6	3.5	5.62
0.02	3	3	-	8	7	8
0.04	3	3	3	10	9	10
0.06	3	3	3	12	10	10
0.08	5	3	3	14	12	10
0.1	6	4	3	18	13	11
0.2	9	8	5	25	22	17
0.3	10	10	8	25	25	22
0.4	10	10	9	26	25	24
0.5	10	10	9	26	25	25
0.6	9	9	10	25	25	26
0.7	9	10	10	25	25	25
0.8	9	9	9	24	25	25
0.9	9	9	9	24	24	25
0.1	8	8	9	23	23	25

some of the values of the cells radius simulated for 5G were not simulated in 4G; the cells of Tab. I indicate the value of R for the $d^{'}_{BP}$ in the 2.6 GHz, 3.5 GHz and 5.62 GHz bands, i.e., 0.156 km, 0.210 km and 0.3372 km respectively. The values of $d^{'}_{BP}\pm 1$ m are also represented.

In Tab. I, the maximum number of supported UTs is shown by cells in yellow. In 4G the maximum number of supported UTs (in yellow) is 10 for all frequency bands. However, at the 2.6 GHz and 3.5 GHz frequency bands, 10 UTs are supported for $0.3 \leq R \leq 0.5$ km. In the 5.62 GHz, 10 UTs are only supported for longer Rs, i.e., $0.5 \leq R \leq 0.7$ km.

For 5G new radio, the maximum supported UTs increases to 26, i.e., 5G new radio (with numerology 0) can supports at the most 16 UTs than 4G. In the 2.6 GHz band, 26 UTs are supported, while at 3.5 GHz 25 UTs are supported and at 5.62 GHz 26 UTs are supported.

IV. Results Beyond Saturation Level

This section analyses results for the behavior of the system in terms of average delay and average goodput after the saturation point. The study of the behavior of the system beyond saturation level is needed to understand how resources are wasted if the service quality requirements are not fulfilled. We need to clearly understand if, for PLR<2% and the 150 ms target delay, identified in [16], the 4G/5G networks are taking full advantage of the available resources, or if the resources are being lost due to QoS degradation.

A. Average Goodput

Fig. 4 presents the average goodput up to and beyond the saturation point. Saturation occurs when PLR<2% is not

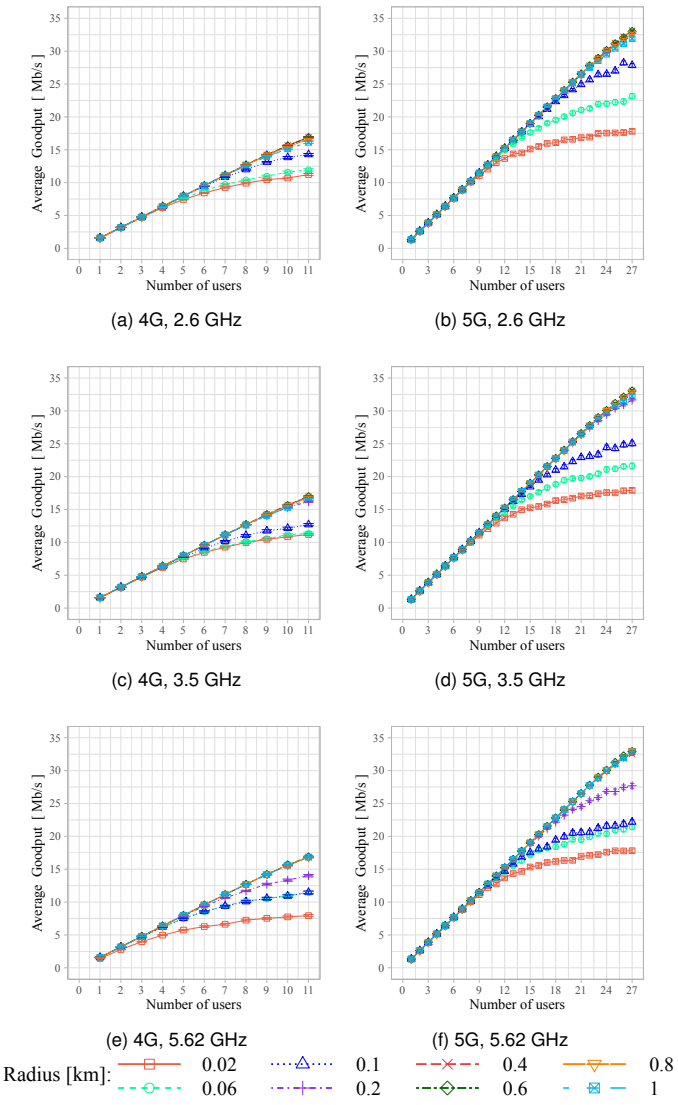

Fig. 4. Results for the average goodput as a function of the number of users, with R as a parameter, for different frequency bands.

verified anymore. While PLR<2%, the average goodput increases linearly[1] with the increase of the number of supported UTs. Beyond this point, when PLR≥2%, while the simulated number of UTs increases, the average goodput curve tends to present a decrease in its slope, and then tends to become almost parallel to the xx axis (horizontal asymptote). We can conclude that for 4G and 5G, although we can add more users beyond the saturation point, the goodput stops to increases and additional UTs only contribute to degrade the overall QoS.

In 4G, the maximum average goodput at the system saturation level is 15.7 Mb/s. With 5G New Radio, it is possible to obtain a maximum goodput of 32.25 Mb/s. Beyond saturation (PLR≥2%), the maximum average goodput for 4G varies between 16.89 Mb/s and 17.01 Mb/s, while in 5G New Radio the maximum average goodput increases up to values between 33 Mb/s and 33.12 Mb/s (for different cell radii).

[1]The saturation point for the average goodput can be determined by drawing vertical lines for the number of users identified in Tab. I (for PLR<2%). The interception point between the vertical line for the given value of R line is the saturation point.

B. Average Delay

The behavior of the average delay as a function of the number of UTs is similar for 4G or 5G New Radio networks, as shown in Fig. 5.

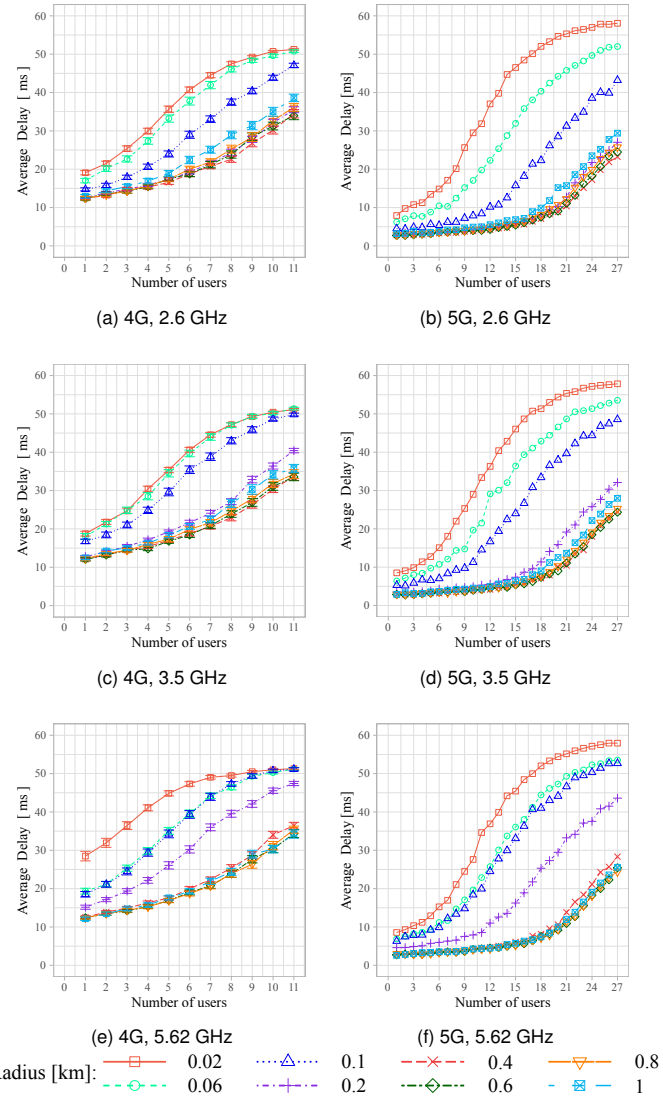

Fig. 5. Results for the average delay as a function of the number of users, with R as a parameter, for different frequency bands.

After the saturation point, the slope of the curves for the average delay first increases, and then decays. After the slope starts to decay the curve becomes almost parallel to the xx axis. This behavior is similar to the one observed for the average goodput. We can than conclude that, beyond saturation, as erroneous packets increase significantly, there is not a significant gain in terms of non-erroneous traffic, and neither goodput nor average delay have a significant increase.

While the maximum obtained average delay for 4G is between 51.27 ms and 51.37 ms, for 5G New Radio it is between 57.95 ms and 58.06 ms (for different cell radii).

It is also worthwhile to note that, up to system saturation, as shown in Fig. 3, the average delay is shorter for 5G New Radio (compared to 4G), while beyond system saturation (Fig. 5), the average delay for 4G and 5G New Radio become closer.

V. Conclusion

We have introduced two urban micro cell scenarios (with 2D versus 3D distances) presented by ITU. These scenarios consider two-slope (TS) path loss models (PLMs), with different implementations in two simulators. Results for LTE-Advanced have been extracted with the LTE-Sim by implementing the UMi cells scenario and underlying PLM. For 5G New Radio, we have considered the 5G-air-simulator and the UMi_A cell scenario (and underlying PLM).

Our study considers three frequency bands (2.6 GHz, 3.5 GHz and 5.62 GHz). The system was taken into saturation, i.e., for a packet loss ratio (PLR) lower than 2% (as defined by 3GPP for video (VID) flows). PLR results are similar across all frequency bands for 4G and to 5G new radio. The shortest cell radius (R) the PLR increases faster with the number of users than for longer Rs. Up to PLR<2% the corresponding values for the average delays are longer in 4G than for 5G. The maximum number of supported users (UTs) is 10 for all frequency bands in 4G. For 5G, in the 2.6 GHz and 5.62 GHz frequency bands, the number of supported users is 26 UTs. For the 3.5 GHz frequency band, it is 25 UTs. Beyond the saturation level (PLR$\geq$2%), the average goodput and average delay did not present a relevant increase, regardless of the number of UTs added. We can conclude that, for video flows, in the considered scenarios, the 3GPP assumption of considering the PLR<2% alone is sufficient to determine the quality of service. This is justified by the fact that results obtained for the average delay in 4G and 5G New Radio are clearly shorter than the 150 ms appointed by 3GPP.

As a suggestion for future work, we intend to explore other packet schedulers for 5G, considering reinforcement learning, in order to increase the number of supported UTs, and consequently system capacity and fairness, without compromise the QoS.

References

[1] Cisco, "Cisco Annual Internet Report (2018–2023) White Paper," Cisco Systems, Inc., Tech. Rep., March 2020. [Online]. Available: https://www.cisco.com/c/en/us/solutions/collateral/executive-perspectives/annual-internet-report/white-paper-c11-741490.pdf

[2] Y. Xu and S. Zhou, "On the Coverage and Capacity of Ultra-Dense Networks With Directional Transmissions," *IEEE Wireless Communications Letters*, vol. 9, no. 3, pp. 271–275, March 2020.

[3] H. Claussen, D. López-Pérez, L. Ho, R. Razavi, and S. Kucera, *Small Cells—The Future of Cellular Networks*. John Wiley & Sons, Ltd, 2017, ch. 1, pp. 1–21. [Online]. Available: https://onlinelibrary.wiley.com/doi/abs/10.1002/9781119307600.ch1

[4] G. Intelligence. (2022) GSMA Intelligence, Data. [Online]. Available: https://www.gsmaintelligence.com/data/

[5] 3GPP, "TS 22.261, Service requirements for the 5G system; Stage 1 (Release 17)," 3rd Generation Partnership Project, Tech. Rep. V17.10.0, March 2022. [Online]. Available: https://www.3gpp.org/ftp/Specs/archive/22_series/22.261/22261-ha0.zip

[6] ——, "TS 22.261, Service requirements for the 5G system; Stage 1 (Release 18)," 3rd Generation Partnership Project, Tech. Rep. V18.6.1, June 2022. [Online]. Available: https://www.3gpp.org/ftp/Specs/archive/22_series/22.261/22261-i61.zip

[7] H. Munir, S. A. Hassan, H. Pervaiz, Q. Ni, and L. Musavian, "Resource Optimization in Multi-Tier HetNets Exploiting Multi-Slope Path Loss Model," *IEEE Access*, vol. 5, pp. 8714–8726, 2017.

[8] T. Daengsi, P. Sirawongphatsara, and P. Pornpongtechavanich, "QoE Modeling Associated with QoS Impairment Parameters in 5G Networks Using AHP Decision Making Technique," in *2021 International Conference on Decision Aid Sciences and Application (DASA)*, Dec. 2021, pp. 550–552.

[9] 3GPP, "TS 22.101, Service aspects; Service principles (Release 17)," 3rd Generation Partnership Project, Tech. Rep. V17.5.0, June 2022. [Online]. Available: https://www.3gpp.org/ftp/Specs/archive/22_series/22.101/22101-h50.zip

[10] ——, "TS 22.101, Service aspects; Service principles (Release 18)," 3rd Generation Partnership Project, Tech. Rep. V18.4.0, June 2022. [Online]. Available: https://www.3gpp.org/ftp/Specs/archive/22_series/22.101/22101-i40.zip

[11] ITU, "Guidelines for evaluation of radio interface technologies for IMT-Advanced," ITU, Tech. Rep. Rep. ITU-R M.2135-1, Dec. 2009. [Online]. Available: https://www.itu.int/pub/R-REP-M.2135-1-2009

[12] ——, "Guidelines for evaluation of radio interface technologies for IMT-2020," ITU, Tech. Rep. Report ITU-R M.2412-0, Nov. 2017. [Online]. Available: https://www.itu.int/dms_pub/itu-r/opb/rep/R-REP-M.2412-2017-PDF-E.pdf

[13] X. Zhang and J. G. Andrews, "Downlink Cellular Network Analysis With Multi-Slope Path Loss Models," *IEEE Transactions on Communications*, vol. 63, no. 5, pp. 1881–1894, 2015.

[14] I. Atzeni, J. Arnau, and M. Kountouris, "Downlink Cellular Network Analysis With LOS/NLOS Propagation and Elevated Base Stations," *IEEE Transactions on Wireless Communications*, vol. 17, no. 1, pp. 142–156, 2018.

[15] C. Galiotto, N. K. Pratas, N. Marchetti, and L. Doyle, "A stochastic geometry framework for LOS/NLOS propagation in dense small cell networks," in *2015 IEEE International Conference on Communications (ICC)*, 2015, pp. 2851–2856.

[16] 3GPP, "TS 22.105, Services and service capabilities (Release 17)," 3rd Generation Partnership Project, Tech. Rep. V17.0.0, March 2022. [Online]. Available: https://www.3gpp.org/ftp/Specs/archive/22_series/22.105/22105-h00.zip

[17] ——, "TS 38.101-1, User Equipment (UE) radio transmission and reception; Part 1: Range 1 Standalone (Release 17)," 3rd Generation Partnership Project, Tech. Rep. V17.5.0, March 2022. [Online]. Available: https://www.3gpp.org/ftp/Specs/archive/38_series/38.101-1/38101-1-h50.zip

[18] M. M. Nasralla, "A Hybrid Downlink Scheduling Approach for Multi-Traffic Classes in LTE Wireless Systems," *IEEE Access*, vol. 8, pp. 82 173–82 186, 2020.

[19] S. Q. Gilani, S. A. Hassan, H. Pervaiz, and S. H. Ahmed, "Performance Analysis of Flexible Duplexing-enabled Heterogeneous Networks Exploiting Multi Slope Path Loss Models," in *2019 International Conference on Computing, Networking and Communications (ICNC)*, Feb. 2019, pp. 724–728.

[20] J. Berg, "A recursive method for street microcell path loss calculations," in *Proceedings of 6th International Symposium on Personal, Indoor qualityand Mobile Radio Communications*, vol. 1, Sep. 1995, pp. 140–143 vol.1.

[21] N. Garg, S. Singh, and J. Andrews, "Impact of Dual Slope Path Loss on User Association in HetNets," in *2015 IEEE Globecom Workshops (GC Wkshps)*, Dec. 2015, pp. 1–6.

[22] G. Piro, L. Grieco, G. Boggia, F. Capozzi, and P. Camarda, "Simulating LTE Cellular Systems: An Open-Source Framework," *IEEE Transactions on Vehicular Technology*, vol. 60, no. 2, pp. 498–513, Feb. 2011.

[23] S. Martiradonna, A. Grassi, G. Piro, and G. Boggia, "5G-air-simulator: An open-source tool modeling the 5G air interface," *Computer Networks*, vol. 173, p. 107151, 2020. [Online]. Available: https://www.sciencedirect.com/science/article/pii/S1389128619317359

[24] R. R. Paulo and F. J. Velez, "LTE-SIM-ITU-R-M.2135-1," https://github.com/RRP-IT/LTE-SIM-ITU-R-M.2135-1.git, 2020.

[25] ——, "5G-air-simulator_ITU-R_M-2412-0," https://github.com/RRP-IT/5G-air-simulator_ITU-R_M-2412-0.git, 2022.